

Solving the Last Mile Problem for Energy

Self-forming Nano-grids

Ben Bacque, Tanya Kirilova Gachovska, Ray Orr,
Nikolay Radimov
Solantro Semiconductor
Ottawa, Canada

David King Li, Shahab Poshtkouhi, Olivier
Trescases
Department of Electrical and Computer Engineering
University of Toronto
Toronto, Canada

Abstract— In the later part of the 1980s, the telephony industry struggled with the cost of connecting subscribers over the last mile to serve millions of people in the developing world. While the cost of switching and transmission lines is shared across hundreds or thousands of subscribers, this advantage diminishes at the edge of the network where the cost must be borne by fewer and ultimately individual subscribers. In power grids today a similar situation exists.

The Last-mile Problem was resolved when the cost of cellular telephones was reduced by integrating functions and components into silicon circuits and when African entrepreneurs found novel financial models to enable even the poorest to acquire a cell phone. Using parallel principles to provide energy where the infrastructure and the required capital investment do not exist, the self-forming nano-grid project discussed in this paper can start from a single photovoltaic (PV) panel and battery each with attached inverters yet scale up to tens of kilowatts. This system also incorporates load management in a power distribution panel to set priority for load shedding to keep critical loads powered in the face of minimal generation and no conventional grid resources.

Keywords—*nano-grid; photovoltaic; power; energy; self-forming; distributed generation; droop control; load shedding.*

I. INTRODUCTION

The International Energy Agency assumes that the initial threshold level of electricity consumption for rural households in Africa is 250 kWh per year and for urban households 500 kWh per year. Today, the average residential electricity consumption per capita for sub-Saharan Africa including South Africa is 317 kWh per year (870 Wh per day). If South Africa is excluded this number drops to 225 kWh per year (616 Wh per day) [1]. A single PV panel and battery can provide this level of power. Direct current solutions are starting to be deployed today for lighting and charging of cell phones. While these solutions provide enormous benefit they are limited in scalability and the range of applications. The ubiquitous plethora of devices that are designed for AC operation, the advantages of simple transformation to higher or lower voltage that Nikola Tesla espoused and the low cost of protection devices such as circuit breakers and fuses continue to make AC electrical systems the default power system.

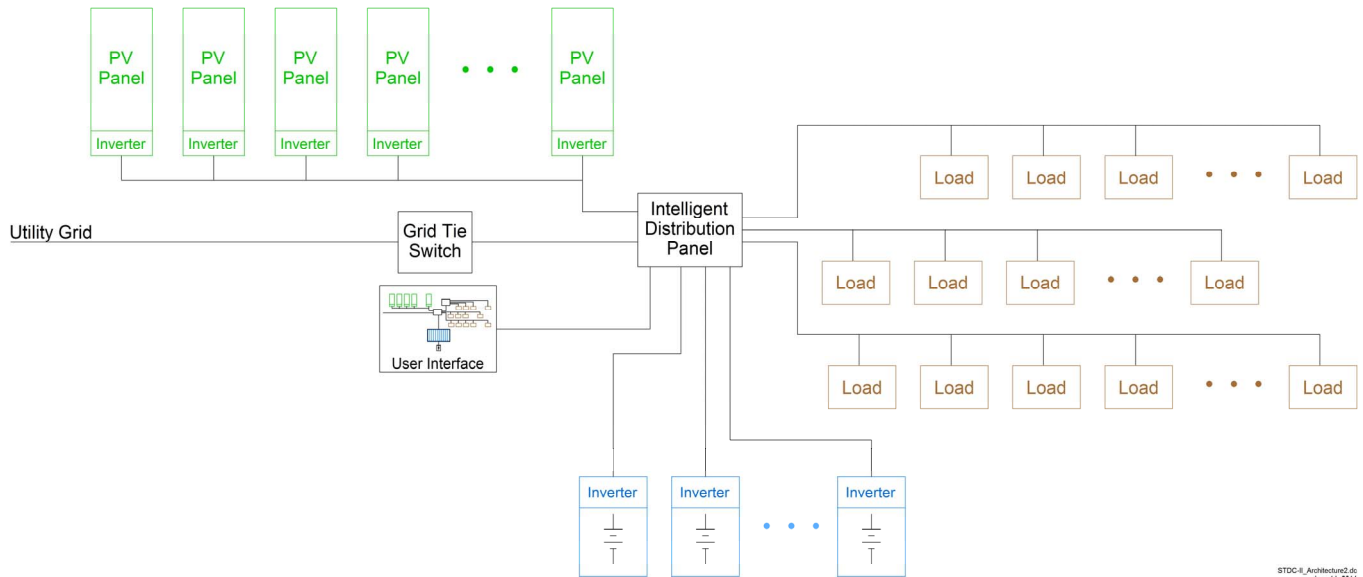
The evolution of energy systems in much of the developing world will not follow the model of large capital investment for generation, transmission and distribution developed countries

have followed. Many countries lack the resources to make investment on a large enough scale to build the infrastructure [1]. The goal of this project is to create an electrical power network that can grow and scale without large capital investments in infrastructure.

Initial efforts in this development involved synthesis and simulation of a range of systems. P-V and Q-f droop mechanisms provides power sharing and management of load shedding and Q sharing respectively. Management of the system is distributed across all inverters and load control elements. Communication provides for longer term grid management such as load priority shifting based on weather conditions and system diagnostic testing. Inverters and intelligent distribution panels have been built based on the requirements determined in system synthesis and simulation. Work continues to build nano-grids for system testing at three field sites. The results thus far suggest one day energy with a very low cost of entry will be provided for the two billion people who do not yet have access to electricity.

II. GRID CONFIGURATION AND CONTROL

To enable scalability and low cost of entry the nano-grid system is configured as a collection of individual PV and battery inverters connected to loads via a distribution panel with load monitoring and control capability as shown in Fig. 1. These elements function cooperatively to form an AC electrical network. The underlying control mechanism is a frequency and voltage droop mechanism as is used in conventional electrical grid control. However, while conventional grids use Q-V and P-f droop relationships [3] we chose an alternate Q-f and P-V relationship because of the non-inductive but highly resistive nature of the very small grids on which we focus and the improved load-sharing characteristics that can be achieved with resistive droop control on these smaller grids [4,5]. These droop relationships are shown in Fig. 2. The internal control of the inverters forces each inverter to behave as a voltage source with a series resistance. The voltage source frequency is varied depending on the reactive power of the grid to follow the Q-f droop relationship. The synthetic source resistance and source voltage are chosen to provide the required P-V droop relationship. All inverters follow the same Q-f relationship shown in Fig. 2 where $+Q_{MAX}$ and $-Q_{MAX}$ are the maximum reactive power Q the inverter is able to source or sink respectively.



STDC-II_Architecture2.00
June 11, 2014

Fig. 1. Self-forming nano-grid system

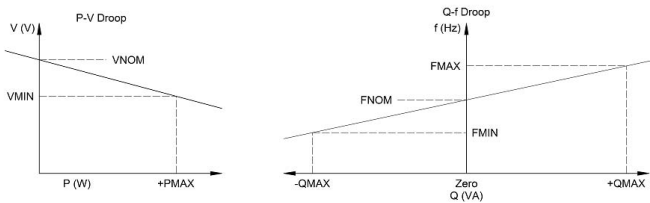


Fig. 2. P-V and Q-f droop relations

The power-voltage relationship differs for PV inverters and battery inverters. PV inverters can only supply power up to the maximum power point, (MPP), of the PV panel. Battery inverters must be able to both supply power to the grid and at another time draw power from the grid to charge the battery. Battery's bidirectional nature and their capability to handle current transients while also serving as storage devices are useful characteristics for controlling the impedance of the grid, providing transient currents for load steps, dumps and start-up and for storage. These characteristics led to the two different control mechanisms for the PV and battery inverters shown in Fig. 3.

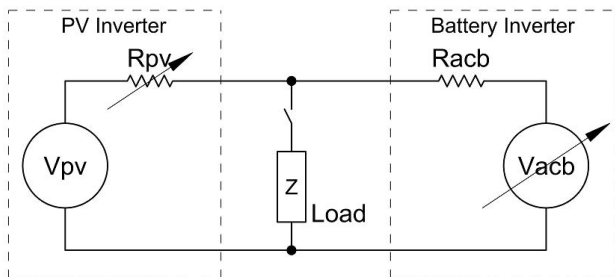


Fig. 3. PV and battery inverter droop control

In this case the PV inverter behaves as a constant voltage source, V_{pv} , with a variable series resistance with the voltage set to the maximum specified for the grid, (264V), and the synthetic resistance, R_{pv} , varying to keep the PV panel at the MPP point. A minimum value of the synthetic resistance causes the PV inverter to back power down from the MPP power when the grid voltage approaches maximum.

For the battery inverter the synthetic resistance, R_{acb} , is fixed in order to limit the grid impedance under light load conditions and to keep the grid voltage within the specified range during transients up to the maximum capability of the inverter. The synthetic source voltage, V_{acb} , is adjusted to supply power to the grid and for charging of the battery.

Load control functions take advantage of the Q-f and P-V droop characteristics as well to shed loads and to determine when they may be reconnected. Table 1 summarizes the behavior of the inverters and the load control panel over the grid voltage range.

Both the PV and battery inverters were designed as two stage power converters. In the case of the battery inverters the first stage is a bidirectional converter that converts power between two potentials: the battery voltage and a value greater than the peak of the AC grid voltage. This converter also limits the current at the grid frequency and harmonics that flows through the battery and provides galvanic isolation of the battery from the grid. In the case of the PV inverter the first stage is a DC to DC converter that provides galvanic isolation of the PV panel from the grid and is controlled to keep the PV panel at the MPP point.

The second stage of both of these inverters is a DC to AC converter constructed from two buck regulators run in anti-phase to generate a differential sinusoid. This architecture was chosen to provide four quadrant operation with the capability

to support current and voltage of either polarity at any instant and bidirectional flow of real and reactive power.

TABLE I. BEHAVIOUR OF INVERTERS AND LOAD CONTROL

	PV generation	Battery charge power	Total Load
V_{Max2} 264VAC	less power than their MPP	being met	less than total supply from generation
V_{Max1} 252VAC	MPP power	not being completely met	equal to total supply from generation
V_{Nom} 240VAC	MPP power if light is available	supplying some or all power to loads.	greater than supply from PV generation.
V_{Min1} 228VAC	MPP power if light is available	supplying some or all power to loads	greater than supply from PV generation. Low priority loads disconnect in this range
V_{Min2} 216VAC	MPP power if light is available, may be current limiting	supplying some or all power to loads, may be current limiting	all loads disconnect in 500 ms or less
$V_{Shutdown}$ 200VAC	stop generation after 2 s ride through	stop generation after 2 s ride through	all loads disconnect in 500 ms or less

III. SIMULATION RESULTS

Simulation cases were developed to test the capability of the system with real and reactive loads, non-linear loads and motor start conditions. Of particular importance in any distributed-generation grid is that the real and reactive power-sharing mechanisms correctly apportion load current (and thus power) to the inverters that can actually deliver that power. Below we show simulation results from a small nano-grid of four 2.5kW PV inverters being subjected to real-power load-steps and load-dumps up to ~6.2kW under varying reactive load conditions and with varying hypothetical insolation levels for each inverter.

The applied real-power load is stepped up and down under zero ($t < 40s$, $t > 120s$), positive ($40s < t < 80s$) and negative ($80s < t < 120s$) reactive power conditions as illustrated in Fig. 4. This test verifies that real power sharing is decoupled from reactive power sharing, and further, that the system is able to bias the power-sharing in order to achieve specific objectives. In this test case, we model inverter #1 as being fully insolated, and wanting to deliver all of its available 2.5kW to the grid throughout the test. Inverter #2 is at half-power. Inverter #3 begins at full power, and linearly declines to zero while inverter #4 does the opposite, increasing from zero to full power. For the last epoch of the test all insolation-levels are set equally.

In Fig. 5 we see the individual inverter real and reactive power delivered to the nano-grid. Observe that as load increases, the lower-insolated inverters deliver only their available power, and inverter #1 is only able to deliver its full power when the real load is at maximum. With equal power-targets in the last epoch, power is equally shared, as expected.

Note that when inverter#1 is delivering its full real power, it is operating at its apparent-power limit, and must begin to shed reactive load if it is to perform its main task of converting real power from the sun: for maximum efficiency, the “natural” power-share function must be biased. One can observe the rapid decline in Q delivered from inverter#1 approaching $t=60s$ in Fig. 5 as an example of this behaviour.

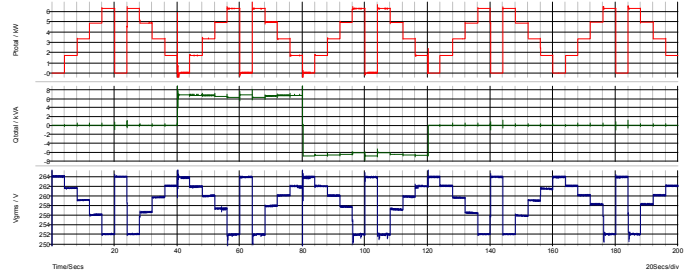


Fig. 4. Test scenario real (top) and reactive (middle) power, RMS grid voltage (bottom)

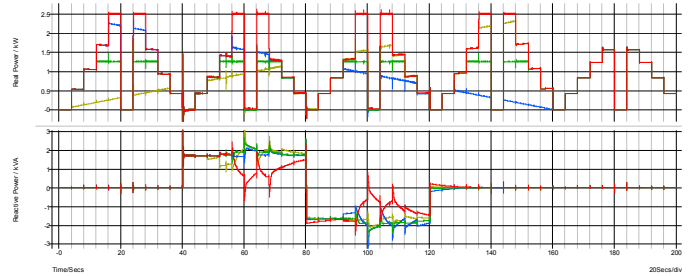


Fig. 5. Individual inverter share of real (top) and reactive power (bottom). Red: inverter1, green: inverter 2, blue: inverter 3, gold: inverter 4

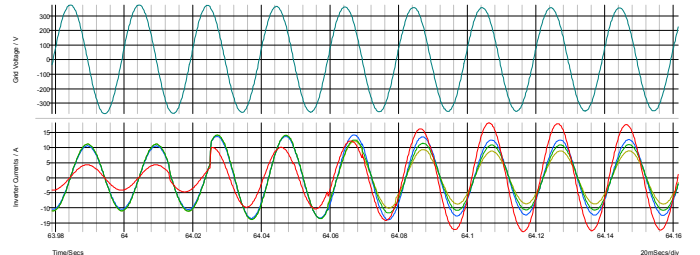


Fig. 6. Real power load-step at $t=64s$: Inverter #1 current-phase rotates to assume greater share of real power. Top: grid voltage, bottom: inverter currents. Red: inverter1, green: inverter 2, blue: inverter 3, gold: inverter 4

We can zoom on the current waveforms to examine in more detail the parallel-system operation. In Fig 6 we can see all the inverters cooperating to deliver the required reactive current. Inverter#1 is delivering less current, as it is still “catching up” from its overload and Q-shed that began at $t=56s$. The real-power load-step hits, and within a few grid cycles the inverters

have all rotated their current-phase so that real power is now delivered, and inverter#1 has rotated furthest and is also delivering the most current, since it has the greatest sunlight.

Fig. 7 shows the opposite, where just before $t=100s$ inverter#1 is delivering the most real power, and its phase is therefore closest to the phase of the grid-voltage. When the entire real load suddenly disappears, it finds its phase at odds with that of the other inverters. But the Q-f droop loop kicks in, and inverter #1 speeds up while the other inverters slow down, resulting in all inverters achieving current-phase lock in about 400mS, at which point inverter #1 begins to ramp up its share of the remaining reactive power.

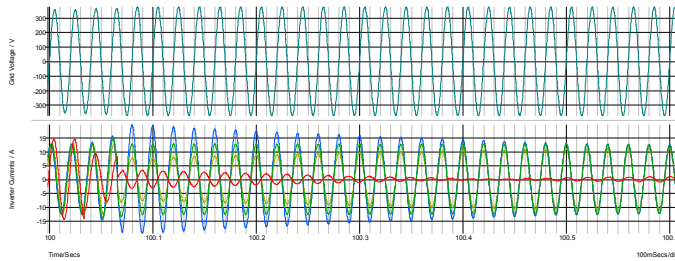


Fig. 7. Real-power load-dump at $t=100s$: Inverter #1 performs 180-degree current-phase rotation to share remaining reactive load. Top: grid voltage, bottom: inverter currents. Red: inverter1, green: inverter 2, blue: inverter 3, gold: inverter 4

IV. TEST RESULTS

PV and battery inverters have been tested to ensure their behaviour under various load conditions. Fig. 8 shows the voltage and current initially with a resistive load and the addition of $5\mu F$ of capacitance at the trigger point. Fig. 9 shows the voltage and current start-up waveforms of an inverter. A range of real, reactive and non-linear loads were used to test the inverters behaviour as a voltage source and to verify the droop characteristics shown in Fig. 2. Testing has begun with multiple inverters in parallel. This testing is the final activity required before building and testing nano-grids at three planned field sites.

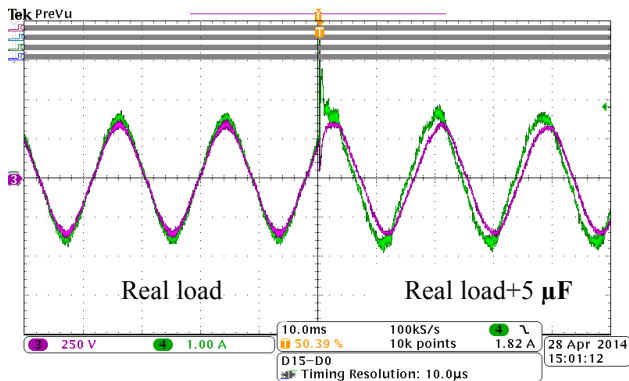


Fig. 8. Grid voltage (magenta) and current (green) for resistive loads and then addition of $5\mu F$ capacitor at the trigger point

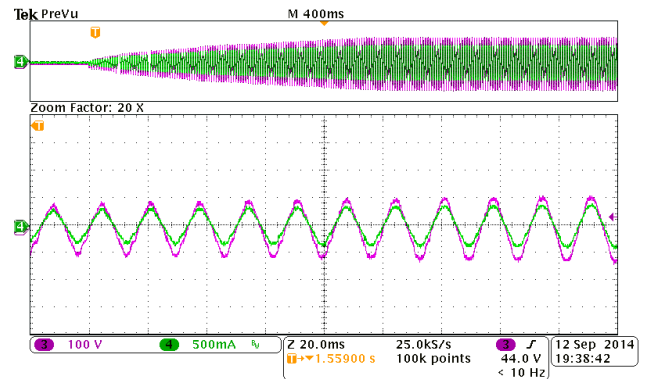


Fig. 9. Grid start-up: voltage (magenta) and current (green)

V. CONCLUSIONS

A scalable, self-forming nano-grid control architecture has been developed and simulated, and is now being implemented in multiple test sites. PV and battery inverters employ synthetic voltage sources connected to form a grid via synthetic resistances. P and Q are shared amongst sources using P-V and Q-f droop mechanisms. This same P-V droop characteristic is used to control load shedding. Simulations and early testing suggest that robust grid can be constructed and scaled by adding individual PV panels, batteries and inverters. Work continues to build and test three of these nano-grid systems.

ACKNOWLEDGMENTS

Solanthro would like to thank Sustainable Development Technology Canada (SDTC) for its support. SDTC is a foundation created by the Government of Canada to support companies in bringing game changing technologies to market which deliver economic and environmental benefits.

REFERENCES

- [1] OECD/EIA 2014 Africa energy outlook pages 29 to 32 <http://www.ica.org/publications/freepublications/publication/africa-energy-outlook.html>
- [2] Saviva Research Review: "Base of the Pyramid Pay As You Go Solar" January 2014 <http://www.savivaresearch.com/wp-content/uploads/2014/01/January-2014-PAYG-Solar-report1.pdf>
- [3] K. De Brabandere, B. Bolsens, J. Van den Keybus, A. Woyte, J. Driesen, and R. Belmans, "A Voltage and Frequency Droop Control Method for Parallel Inverters," *35th Annual IEEE Power Electronics Specialists Conference*, Aachen, Germany, 2004, pp 2501-2507.
- [4] J. M. Guerrero, J. Matas, L. Garcia de Vicuña, M. Castilla, and J. Miret, "Decentralized control for parallel operation of distributed generation inverters using resistive output impedance," *IEEE Trans. Ind. Electron.*, vol. 54, no. 2, April 2007, pp. 994-1004.
- [5] T. L. Vandoorn, J. D. M. De Kooning, B Meersman, J.M. Guerrero, L. Vandevelde, "Automatic Power Sharing Modification of P/V Droop Controllers in Low-Voltage Resistive Microgrids," *IEEE Transactions on Power Delivery*, vol. 27, no.4, October 2012, pp. 2318-2325.